High Sensitivity Polyvinylidene Fluoride Microphone Based on Area Ratio Amplification and Minimal Capacitance

Jian Xu, Leon M. Headings, and Marcelo J. Dapino

***Abstract*— This paper presents an inexpensive high-sensitivity microphone based on polyvinylidene fluoride (PVDF) film. High sensitivity is achieved through pressure amplification created by the area ratio between the rigid surface exposed to acoustic waves and a crosshair-shaped PVDF film, in combination with the reduced capacitance created by a similarly shaped top electrode. The crosshair shape is obtained through simple chemical etching from commercial PVDF film. Finite-element simulations including static structure analysis, modal analysis, and harmonic response are performed to design the microphone. Peak coalescence of the first three adjacent natural frequencies caused by the structure damping ratio is observed. Static and dynamic stress analyses ensure that the design meets the mechanical constraints imposed by PVDF. A plane wave tube experiment and signal conditioning electronics are developed. Measurements include benchmarking against a commercial microphone and show that the PVDF microphone exhibits a linear response up to a sound pressure level of 140 dB and overall fluctuations of less than ±4 dB over the frequency range of 10 to 20 000 Hz. The sensitivity of the microphone alone, without a conditioning circuit, is measured as 27.8 μV/Pa, which is 3.01 times the sensitivity of commercial PVDF film operating in 3-3 mode. This sensitivity gain is close to the physical area ratio of 3.2. We experimentally characterize the directivity of the sensor and measure a decay of −10.5 dB at ±90° from the microphone's axis.**

***Index Terms*— PVDF, microphone, crosshair, peak coalescence, plane wave, notch filter.**

I. Introduction

THIS paper addresses the development of compact and inexpensive microphones capable of high sensitivity and broad frequency response. The principle for designing these microphones is based on polyvinylidene fluoride (PVDF), a polymer that is mechanically and chemically robust, flexible, and lightweight. In its β phase, PVDF exhibits ferroelectric properties including high sensitivity to stress which results in the generation of charge when the material is stressed. Compared to piezoceramics such as lead zirconate-titanate (PZT), PVDF can generate 10−25 times greater voltages for the same pressure input [1], [2].

The piezoelectricity of PVDF was first discovered in 1969 [3] and has since been developed for sensors in a wide range of military, industrial, and biomedical applications [4]–[7]. These polymers are resistant to moisture, most chemicals, oxidants, and intense ultraviolet and nuclear radiation [1], [8]. PVDF is synthesized by addition polymerization of the $CH_2 = CF_2$ monomer, and exhibits α, β, γ, and δ phases. The α phase is non-polar and the lowest energy form. The γ and δ phases are not common. The β phase has a net dipole moment that points from the electronegative fluorine to the electropositive hydrogen and is nearly normal to the polymer chain [9], [10].

Sensors based on PVDF film are attractive due to their high sensitivity and low cost. Such sensors are critical for developing accurate noise prediction tools and noise suppression techniques for various applications such as aeroacoustic measurements and cardiorespiratory monitoring.

Arnold et al. [11] designed and tested a piezoresistive silicon microphone for aeroacoustic measurements that improved upon a similar design to lower the noise floor and reduce drift. This design used four single crystal silicon piezoresistors located around the perimeter of a silicon nitride diaphragm and produced a sensitivity of 1.66 μV/Pa with a dynamic range of 52 dB to 160 dB and an average sensitivity drift of ±0.6 dB. This piezoresistive microphone was later integrated into a low-cost directional acoustic array [12]. For providing self-powered aeroacoustic measurements, Horowitz et al. [13] designed and tested a micromachined piezoelectric microphone. This microphone used an annular ring of PZT deposited on a silicon diaphragm and provided a sensitivity of 1.66 μV/Pa with a dynamic range of 35.7–169 dB and a resonant frequency of 59.0 kHz.

Wang et al. [14] designed a piezoelectric microacoustic sensor using a PZT laminate beam with interdigitated electrodes and in-plane polarization. Compared to more common parallel-plate electrodes and through-thickness polarization, this in-plane design provides much higher sensitivity due to the reduced capacitance and design flexibility provided by the interdigitated electrodes. It also capitalizes on the larger piezoelectric stress constant g_{33} compared to g_{31}.

PVDF film pressure sensors have been developed for medical applications such as in-sleep cardiorespiratory

Manuscript received October 29, 2013; accepted November 20, 2014. Date of publication December 10, 2014; date of current version March 27, 2015. This work was supported in part by the Smart Vehicle Concepts Center and in part by the National Science Foundation through the Industry/University Cooperative Research Center Program Evaluation Project. The associate editor coordinating the review of this paper and approving it for publication was Prof. Zeynep Celik-Butler. *(Corresponding author: Marcelo J. Dapino.)*

The authors are with the Department of Mechanical and Aerospace Engineering, The Ohio State University, Columbus, OH 43210 USA (e-mail: xu.212@osu.edu; headings.4@osu.edu; dapino.1@osu.edu).

Color versions of one or more of the figures in this paper are available online at http://ieeexplore.ieee.org.

Digital Object Identifier 10.1109/JSEN.2014.2379636

monitoring [15]. Electronic stethoscopes are used for sensing lung sounds which, using various data processing techniques, can be used to identify abnormal respiratory behaviors [16], [17]. While electronic stethoscope arrays are of great interest due to their non-invasive nature, the size of existing electronic stethoscopes (typically 25 mm diameter) prevents their use in small sound fields in infants and small children. This presents an opportunity for high sensitivity PVDF sensors. Toda et al. [18] developed a PVDF contact vibration sensor with better low frequency performance than conventional electronic stethoscopes. The design uses a concave PVDF film with a rubber contact head to transmit vibrations from the skin and provides a flat frequency response from 16 Hz to 3 kHz.

Xu et al. [19] presented a miniature microphone with micron-sized PVDF pillars manufactured using photolithography techniques. The microphone achieves over 40 times the sensitivity of bulk PVDF film using two design principles: increasing the charge generated for a given input pressure and decreasing the device capacitance. Because PVDF responds to stress, the charge output can be increased by increasing the stress on the PVDF for a given input pressure. This can be achieved if a rigid membrane that is exposed to acoustic waves is used to transmit the sound pressure to a reduced PVDF area. In the micro-pillar design, the charge is amplified by the area ratio between the membrane and the combined area of the micro-pillars. For the second design principle, the voltage output is increased by decreasing the capacitance using shaped electrodes to cover only the active PVDF area. In the micro-pillar design, the invidual round electrodes at the tops of the micro-pillars are connected using thin conducting tabs and a continuous electrode is used underneath the micro-pillar array. The device capacitance is reduced by excluding the capacitance of the air between the micro-pillars.

In this paper, we greatly simplify the manufacture of PVDF sensors exploiting the design principles developed by Xu et al. [19]. Instead of using polydimethylsiloxane (PDMS) stamps molded from photolithographically fabricated masters, we chemically etch the inactive electrode areas using a simple metallic mask. For demonstration purposes, a crosshair electrode shape is presented. We show that the microphone exhibits a linear response up to a sound pressure level (SPL) of 140 dB and overall fluctuations of less than ± 4 dB over 10 to 20 000 Hz. The sensitivity of the microphone alone, without a conditioning circuit, is found to be 27.8 μV/Pa, which is 3.01 times the sensitivity of commercially available PVDF film used in 3-3 mode. This sensitivity gain is close to the physical area ratio of 3.2. We experimentally characterize the directivity of the sensor and obtain a decay of -10.5 dB at 90 degrees from the microphone's axis.

II. Design and Fabrication of the Crosshair Shaped PVDF Microphone

Figure 1 shows the fabrication process for the patterned PVDF microphone. An aluminum pattern is placed firmly on top of a 28 μm thick silver ink metalized polarized PVDF film (1-1004346-0, Measurement Specialties, Inc., USA) by applying M-Bond 200 adhesive

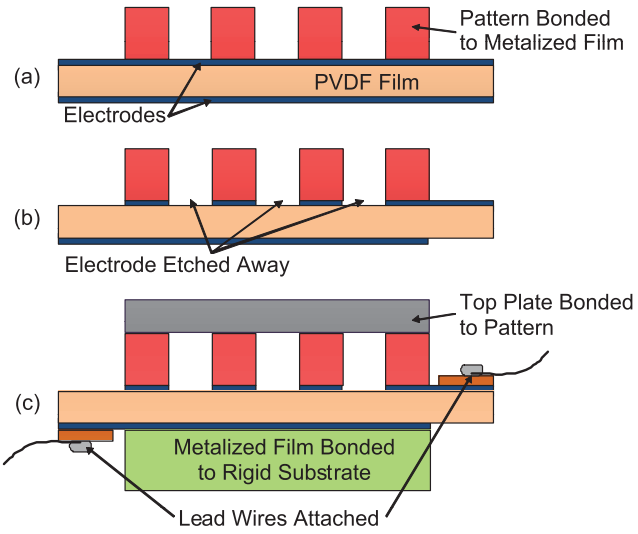

Fig. 1. Etch-based fabrication process for a patterned PVDF microphone: (a) an aluminum pattern is bonded to the metalized film, (b) electrodes are etched away in the inactive area, and (c) a rigid top plate is bonded to the top of the pattern, lead wires are attached, and the bottom surface of the PVDF assembly is bonded to a rigid substrate.

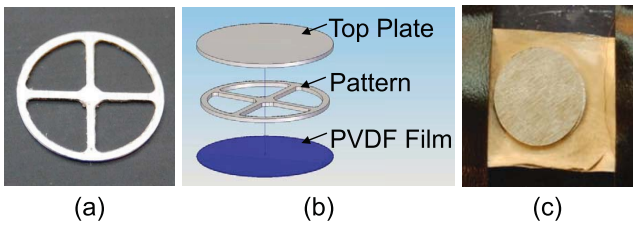

Fig. 2. (a) Photograph of the aluminum crosshair pattern; (b) exploded view of the assembly; and (c) photograph of the assembled microphone.

(Vishay Micro-Measurements, USA) to the bonding surface between them, Figure 1(a). Next, acetone is used to etch away the electrodes of the inactive area as shown in Figure 1(b). The sensitive area of the microphone is formed by overlapping isolated electrodes from both sides. Third, a rigid membrane is bonded (also using M-Bond 200) on top of the pattern to be subjected to external pressure, Figure 1(c). Two conductive-adhesive coated copper foil tapes (3M 1181) with the wires previously soldered on the surface are adhered to the top and bottom electrodes of the PVDF film. The bottom surface of the crosshair PVDF assembly is then bonded to a rigid substrate material.

The pattern can be made using various techniques such as milling, laser cutting, and photolithography, which makes this process flexible and simple. In general, the higher resolution of laser cutting and photolithography enables a larger area ratio than CNC-milling. The crosshair pattern is made in three steps: 1) a CAD model of the crosshair pattern is developed in Solid Edge; 2) the CAD model is imported into FeatureCAM to generate CNC G-code based on user settings; and 3) the G-code is loaded into a Sherline Model 2000 vertical mill combined with a FLASHCUT CNC controller and implemented to fabricate the aluminum alloy pattern. The crosshair pattern, shown in Figure 2(a), was produced with an area of about 17.733 mm^2 and a thickness of 0.254 mm. A circular aluminum alloy top plate with a diameter of 8.5 mm (area of 56.745 mm^2) and a

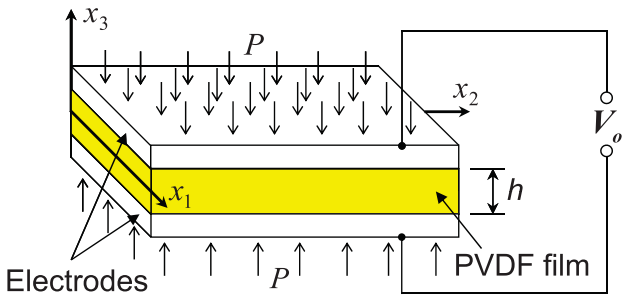

Fig. 3. Open circuit schematic of PVDF film with a pressure P applied uniformly over both top and bottom electrodes.

thickness of 0.254 mm was CNC machined in the same way. Therefore, the area ratio between the top plate and the pattern is 3.2. After the crosshair pattern and top plate were obtained, the microphone was fabricated by the process described above and in Figure 1. If NiCu alloy metalized PVDF film is used, other etchants such as ferric fluoride solvent can be employed to dissolve the electrodes.

III. Sensitivity Analysis

The static sensitivity K is defined as the ratio of the PVDF output voltage V_o over the pressure P acting on the sensor surface,

$$K = V_o/P. \tag{1}$$

The sensitivities of three PVDF sensor designs are compared: flat continuous film, crosshair PVDF microphone with full electrodes, and crosshair PVDF microphone with shaped electrodes.

A. Flat Continuous PVDF Film

Figure 3 shows the open circuit of a flat PVDF film sensor with a uniformly applied pressure. The open circuit voltage generated across the film thickness is

$$V_o = -g_{33}\, h\, \sigma, \tag{2}$$

where g_{33} is the piezoelectric stress constant in the x_3-direction, h is the thickness of the PVDF film, and σ is the stress induced in the material. For a uniformly applied pressure, $\sigma = P$ and substitution of (2) into (1) gives the sensitivity as

$$K_1 = -g_{33}\, h. \tag{3}$$

B. Crosshair PVDF Microphone With Full Electrodes

Here, the crosshair PVDF microphone with full electrodes is analyzed. In this case, the crosshair shape acts to amplify stress but, without using patterned electrodes, the charge induced in the material is distributed over the full electrodes. The charge output by the sensor corresponds to the charge generated by the active area (i.e., the area of the crosshair pattern),

$$Q = Q_{ch} \equiv C_{ch}\, V_{ch}, \tag{4}$$

where Q is the total charge collected at the electrodes, Q_{ch} is the charge generated in the crosshair area, C_{ch} is the capacitance in the crosshair area, and V_{ch} is the potential in the crosshair area. The capacitance is, by definition,

$$C_{ch} = \varepsilon \frac{A_{ch}}{h}, \tag{5}$$

where ε is the permittivity of PVDF and A_{ch} is the total cross-sectional area of the crosshair pattern. According to the linear constitutive piezoelectric equations, the voltage output is proportional to the stress in the active PVDF area. The stress in the PVDF crosshair area due to the application of a normal pressure on the sensor top-plate surface is

$$\sigma_{ch} = \alpha\, P, \tag{6}$$

where α is the area ratio between the circular top-plate and the crosshair pattern. From (2) where $\sigma = \sigma_{ch}$, the voltage generated in the active crosshair area is then

$$V_{ch} = -g_{33}\, h\, \alpha\, P. \tag{7}$$

So, using (5) and (7), the total charge collected at the electrodes can be written from (4)

$$Q = Q_{ch} = -\alpha\, \varepsilon\, A_{ch}\, g_{33}\, P. \tag{8}$$

The total capacitance is the sum of the capacitance of the active area and the capacitance of the inactive area

$$C_t \equiv C_{ch} + C_{in} = \alpha\, \varepsilon \frac{A_{ch}}{h}, \tag{9}$$

where C_{in} is the capacitance of the inactive area. Since the two capacitances are connected in parallel, the voltage drop is the same across the active and inactive areas,

$$V_o = \frac{Q}{C_t}. \tag{10}$$

Combining (1) and (8)–(10) gives the sensitivity of the crosshair PVDF with full electrodes as

$$K_2 = -g_{33}\, h. \tag{11}$$

Hence, the sensitivity of the crosshair PVDF microphone with full electrodes is equal to that of the flat continuous PVDF film with a uniformly applied pressure. The sensitivity amplification ratio, defined as the sensitivity relative to that of the flat continuous PVDF film (K_2/K), is therefore 1. Although the stress is amplified by the effect of the area ratio, the microphone also contains an inactive electrode area which contributes an additional capacitance. The charge induced by the active area has to be distributed over the two capacitances, which reduces the overall voltage. These effects cancel each other out.

C. Crosshair PVDF Microphone With Patterned Electrodes

In this case, the electrodes are patterned to match the crosshair pattern. This may be achieved using the etching method outlined in Section II. Both the capacitance and the charge are due solely to the crosshair pattern, hence the sensitivity is given by (1), (8), and (10), where C_{in} is zero and $C_t = C_{ch}$ (5). The sensitivity therefore has the form

$$K_3 = \alpha(-g_{33}\, h), \tag{12}$$

which increases monotonically with the area ratio α. The sensitivity amplification ratio K_3/K is therefore equal to the area ratio. In theory, the sensitivity of the crosshair PVDF microphone with patterned electrodes can be increased by increasing the area ratio as high as manufacturing and electrical circuit constraints allow. The active area and corresponding charge output (8) must be sufficient for the input impedance of the electronics connected to the PVDF electrical output signal.

In a previous article [19], two designs were proposed: PVDF micro-pillars with patterned electrodes and with full electrodes. Unlike the crosshair PVDF microphone where the area amplification occurs using a rigid membrane over a crosshair pattern on a uniform PVDF film, the PVDF micro-pillar design uses a rigid membrane directly over PVDF micro-structures. The sensitivity of PVDF micro-pillars with patterned electrodes was shown to have the form

$$K_{m3} = \left[\frac{(d+g_1)(d+g_2)}{\pi\, d^2/4}\right](-g_{33}\, h), \tag{13}$$

while the sensitivity of PVDF micro-pillars with full electrodes is

$$K_{m2} = \left[\frac{\varepsilon_r (d+g_1)(d+g_2)}{(\pi\, d^2/4)(\varepsilon_r - 1) + (d+g_1)(d+g_2)}\right](-g_{33}\, h). \tag{14}$$

Here, d is the diameter of each micro-pillar, g_1 and g_2 are the gaps between pillars in the x and y directions, h is the height of the pillars, and ε_r is the relative permittivity of PVDF film. Therefore, compared with the flat continuous PVDF film (3), the sensitivity amplification ratios of PVDF micro-pillars with patterned electrodes and with full electrodes equal the bracketed terms in (13) and (14), respectively.

It is noted that the bracketed term in (13) represents the area ratio of the micro-pillar pattern. Therefore, the crosshair PVDF microphone with shaped electrodes and the PVDF micro-pillar microphone with shaped electrodes both have the same sensitivity if the area ratios are equal and the transverse stress from the surrounding materials in the former case is neglected (relatively small compared with the normal stress). While the crosshair PVDF microphone with full electrodes has a sensitivity amplification ratio of 1, the micro-pillar PVDF microphone with full electrodes has a sensitivity amplification ratio that is always greater than 1. This is due to the inclusion of air between the electrodes in the crosshair PVDF microphone with full electrodes, which has a lower permittivity than bulk PVDF film. However, in contrast to PVDF micro-pillars with shaped electrodes which have a sensitivity amplification ratio that is strictly increasing with increasing geometry ratio g/d (letting $g = g_1 = g_2$), the relative sensitivity of PVDF micro-pillars with full electrodes is limited by the relative permittivity of PVDF film ($\varepsilon_r \sim 12$) as g/d goes to infinity. The designs with patterned electrodes exclude the capacitance of the inactive area, whether it consists of air or PVDF film.

IV. Finite Element Analysis

Considering a potential target frequency bandwidth of 100 kHz and dynamic range (SPL) of 180 dB, finite element simulations including static structure analysis, modal analysis, and harmonic response are performed in ANSYS WORKBENCH to design and analyze the crosshair pattern PVDF microphone assembly. The microphone assembly consists of three components (top circular plate, crosshair pattern, and PVDF film) which are imported into ANSYS. The boundary between the top plate and the crosshair pattern is assumed to be perfectly bonded, as is the interface between the crosshair pattern and the PVDF film. The bottom surface of the PVDF film is fixed.

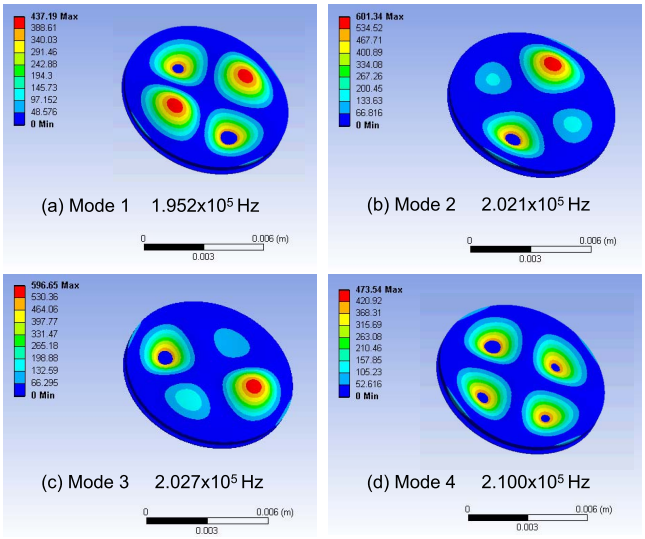

Fig. 4. ANSYS calculation of the first four mode shapes of the microphone assembly.

A modal analysis is performed to confirm that modal resonances of the microphone assembly occur above the targeted 100 kHz bandwidth. Figure 4 shows the mode shapes of the first four resonant modes of the microphone assembly as predicted by ANSYS. These first four modes correspond to resonances of the top plate. Typically, the fundamental mode is of interest because it determines the frequency bandwidth of the system. However, in this design, the first four natural frequencies are very close (Figure 4) and therefore it is necessary to study and analyze the first four modes. The first mode, with two pairs of poles moving out-of-phase, has a predicted resonant frequency of 195.2 kHz while the fourth mode, consisting of in-phase motion of the four poles, has a predicted resonant frequency of 210.0 kHz. Due to the symmetry of the design, the mode shapes of the second mode and the third mode are 90-degree symmetric. The predicted natural frequencies are 202.1 kHz and 202.7 kHz, respectively. The small difference could be due to CAD model conversion, mesh, and calculated errors.

Next, a harmonic response analysis is performed to examine the mechanical response up to the targeted 100 kHz bandwith. An SPL of 180 dB is applied normal to the aluminum top plate and the same boundary conditions as described above are used. According to the existing literature [20], commercial PVDF film has a damping ratio of around 1.7% while the damping ratio of aluminum structures is approximately 2%. A damping ratio of 2% for the complete assembly is chosen

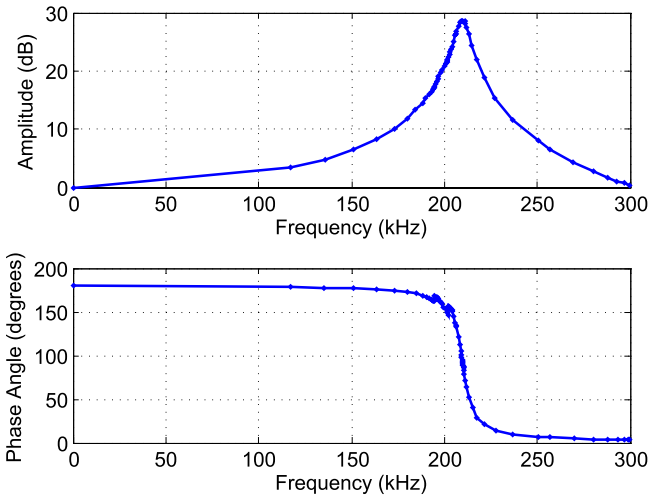

Fig. 5. Calculated frequency response of displacement for the microphone assembly with a damping ratio of 2%.

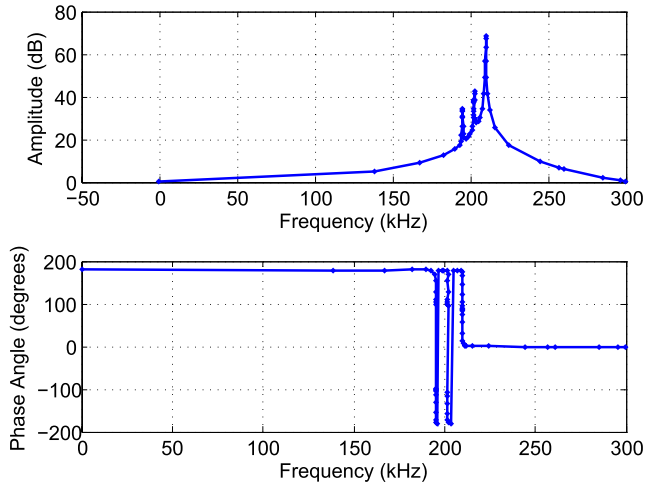

Fig. 6. Calcuated frequency response of displacement for the microphone assembly with a damping ratio of 0.02%.

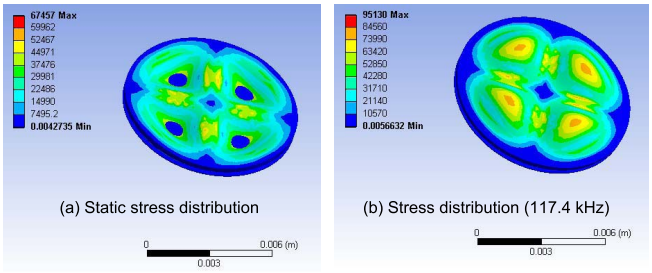

Fig. 7. (a) ANSYS calculation of the static stress distribution over the microphone assembly at an SPL of 180 dB. The maximum static stress is 67.46 kPa. (b) Harmonic stress distribution over the microphone assembly at 117.4 kHz and an SPL of 180 dB. The maximum dynamic stress is 95.13 kPa.

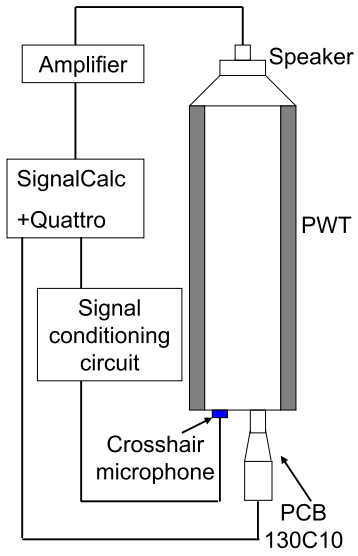

Fig. 8. Schematic of the experimental setup used for characterization and benchmarking of the PVDF microphone.

for this simulation. As shown in Figure 5, the amplitude gain relative to the quasi-static amplitude of $2.63e^{-9}$ m is less than 3 dB over 0–100 kHz, with a phase change of less than 3 degrees over that frequency range. Peak coalescence is observed due to three close natural frequencies. There are two main factors that can lead to peak coalescence: one is calculation resolution of a simulation or frequency resolution of a measurement system, and the other is a system with significant damping that causes adjacent resonant peaks to become coupled. In order to investigate peak coalescence in this case, the simulation is run for a damping ratio of 0.02%. As shown in Figure 6, two additional peaks appear relative to the 2% damping case, which verifies that the peak coalescence of this structure is associated with damping.

Mechanical strength must also be considered for the microphone assembly design. A static FE analysis is conducted to study the stress distribution over the microphone assembly. Figure 7(a) shows the static stress distribution over the microphone assembly with an SPL of 180 dB applied perpendicular to the surface of the top aluminum plate. The maximum equivalent (von Mises) stress is found to be 67.46 kPa, which is much smaller than the yield strengths of the PVDF film (45−55 MPa) and the aluminum alloy (∼280 MPa). Since the microphone is operated under dynamic pressure conditions, the harmonic stress distribution is analyzed under an SPL of 180 dB at 117.4 kHz. The resulting dynamic stress distribution is shown in Figure 7(b), with a maximum dynamic stress of 95.13 kPa. This maximum dynamic stress is larger than the maximum static stress, but is still much smaller than the yield strengths of the two materials.

V. Experimental Setup and Results

The experimental setup shown in Figure 8 is developed to conduct various acoustic tests including relative sensitivity response, sensitivity calibration, and sensor linearity. To calibrate the dynamic response of the microphone, a speaker is attached to one end of a circular plane wave tube (PWT). The speaker is driven by a sinusoidal wave or band-limited white signal generated by a DataPhysics ACE Quattro data acquisition system and SignalCalc software. A commercial microphone, PCB 130C10, is used as

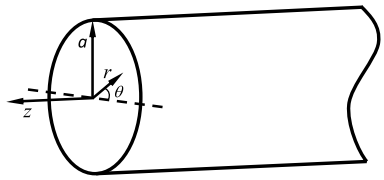

Fig. 9. Infinite circular tube with radius a.

the reference. The crosshair microphone is placed next to the commercial microphone at the opposite end of the PWT. A PWT is used to propagate only the fundamental mode (0, 0) plane wave and ensure that the higher order modes are damped for various acoustic tests. The signals from the crosshair microphone are processed by a signal conditioning circuit and fed into the data acquisition system while the signals from the commercial microphone are recorded and analyzed by the same data acquisition system using its ICP-coupled interface.

A. Circular Plane Wave Tube Design

Assuming an infinite rigid-walled tube as shown in Figure 9, the linearized wave equation for the propagation of acoustical waves in cylindrical coordinates can be expressed in the form [21], [22]

$$\nabla^2 \phi(r,\theta,z,t) = \frac{1}{c_0^2}\,\frac{\partial^2 \phi(r,\theta,z,t)}{\partial t^2}, \tag{15}$$

where ∇^2 is the Laplace operator, ϕ is velocity potential, and c_0 is speed of sound. With $\phi(r,\theta,z,t) = \phi'(r,\theta,z)\,e^{j\omega t}$, the Helmholtz equation results,

$$\nabla^2 \phi'(r,\theta,z) = -k^2\,\phi'(r,\theta,z), \tag{16}$$

i.e.,

$$\frac{\partial^2 \phi'}{\partial r^2} + \frac{1}{r}\,\frac{\partial \phi'}{\partial r} + \frac{1}{r^2}\,\frac{\partial^2 \phi'}{\partial \theta^2} + \frac{\partial^2 \phi'}{\partial z^2} + k^2\,\phi' = 0, \tag{17}$$

where k is wave number (ω/c_0) and ω is angular frequency. Using separation of variables, $\phi'(r,\theta,z) = R(r)\,\Theta(\theta)\,Z(z)$, and solving the three ordinary differential equations yields the general solution

$$\phi(r,\theta,z,t) = [A_r\,J_m(k_r\,r) + B_r\,N_m(k_r\,r)][A_\theta\,e^{-jm\theta} + B_\theta\,e^{jm\theta}][A_z\,e^{-jk_z z} + B_z\,e^{jk_z z}]e^{j\omega t}, \tag{18}$$

where $k_z^2 = k^2 - k_r^2$; J_m and N_m are m-order Bessel and Neumann functions, respectively.

Next, boundary conditions for a tube can be applied to (18). Since $N_m(k_r\,r \to 0) \to -\infty$ and ϕ has to be finite at $r = 0$, then $B_r = 0$. At $r = a$, the rigid wall condition dictates that the particle velocity u_r equals zero. Thus,

$$u_r = \frac{\partial \phi}{\partial r}|_{r=a} = A_r\,k_r\,J_m'(k_r\,a) = 0. \tag{19}$$

The solution of (19) is

$$k_{rmn}\,a = \alpha_{mn}, \tag{20}$$

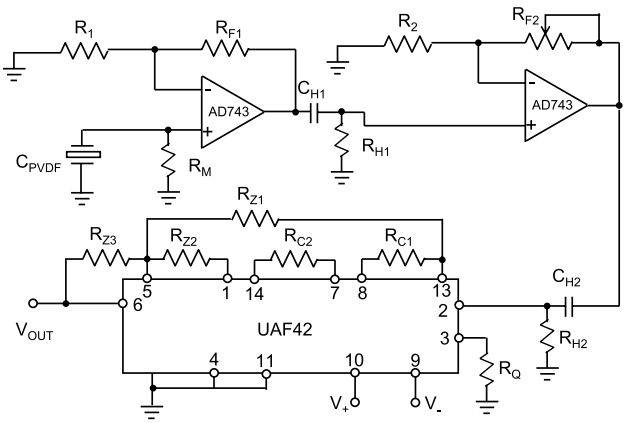

Fig. 10. Schematic diagram of signal conditioning circuit.

where α_{mn} represents the root of the Bessel function and m and n represent the diametral and radial mode numbers, respectively. Therefore, the total solution can be written in the form

$$\phi(r,\theta,z,t) = \sum_{m=0}^{\infty}\sum_{n=0}^{\infty} A_r\,J_m\left(\alpha_{mn}\,\frac{r}{a}\right)\left[A_\theta\,e^{-jm\theta} + B_\theta\,e^{jm\theta}\right] \times\left[A_{zmn}\,e^{-jk_{zmn}z} + B_{zmn}\,e^{jk_{zmn}z}\right]e^{j\omega t}, \tag{21}$$

where $k_{zmn}^2 = k^2 - (\frac{\alpha_{mn}}{a})^2$. Parameter k_{zmn} must be real-valued for wave propagation to occur; otherwise, if k_{zmn} is imaginary, the (m, n) mode waves are damped exponentially along the tube length. Therefore, propagation of only plane waves, mode (0, 0), requires that all higher order modes are damped

$$k < \frac{\alpha_{10}}{a}. \tag{22}$$

Values of α_{mn} can be found in tables of Bessel function roots [21], where the smallest root is $\alpha_{10} = 1.841$. Assuming $c_0 = 343$ m/s, substitution of $k = \frac{2\pi f_c}{c_0}$ into (22) gives

$$a < \frac{100.5}{f_c}, \tag{23}$$

where f_c is the cut-off frequency of the circular tube and represents the highest allowable characterization frequency. For instance, for $f_c = 20$ kHz, then $a < 0.0051$ m. Calibration tests at frequencies less than 2 kHz require $a < 0.0503$ m. In addition, far field wave excitation requires that $k\,l \gg 1$, where l is the tube length. If the microphone is calibrated at 1 kHz, $l \gg 0.0546$ m. For simplicity, a tube length of 1 m is used for all acoustic tests.

B. Signal Conditioning Circuit

Figure 10 shows the signal conditioning circuit developed for the PVDF crosshair microphone. It consists of a buffer circuit with two operational amplifiers in series, two high-pass RC filters, and a 60 Hz notch filter. The output of piezoelectric sensors can be amplified using either charge or voltage amplifiers. For charge amplifiers, the output voltage is equal to Q_0/C_f, where Q_0 is the charge generated and C_f is the capacitance of the feedback capacitor.

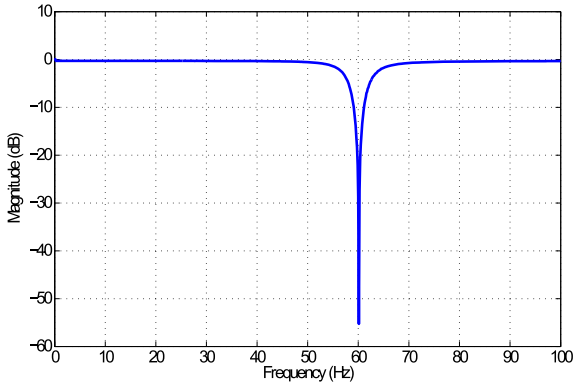

Fig. 11. Magnitude of the measured response of the 60 Hz notch filter.

Therefore, the output voltage does not depend on the sensor capacitance and large output voltages can be generated by using a small feedback capacitance. However, the feedback capacitance causes filtering effects at high frequencies, making charge amplifiers impractical above 50 kHz. As a result, a voltage amplifier is used in our signal conditioning circuit.

The load resistance in a voltage amplifier would load the high impedance output of the PVDF and result in a decreased voltage. In order to prevent this loading effect, a buffer circuit can be used to convert the high output impedance signal into a low impedance signal. An operational amplifier such as the Analog Devices AD743 provides a very high input resistance (300 GΩ) and small output resistance (around 10 Ω). A first-order high-pass filter after the output of each operational amplifier is also used to decouple DC voltage and low frequency components generated by thermal effects. This is useful to avoid the potential for signal drift and saturation of the amplifier. Therefore, the first amplifier gain (R_{F1}/R_1) should be smaller than that of the second amplifer (R_{F2}/R_2). A total gain of 1000 is used for the acoustic tests.

Powerline frequency is a key source of noise for this and other PVDF film-based microphones. One effective solution to this problem is a 60 Hz notch filter. A notch filter can eliminate the 60 Hz noise while not degrading the measurement signal. A filter with a notch frequency of 60 Hz and quality factor Q of 10 is realized with a UAF42 chip and six external resistors (Figure 10). Here, $R_{C1} = R_{C2} = 2.65$ MΩ is calculated as $1/(2\pi\ f_o\, C)$, where f_o is the notch frequency of 60 Hz and C is the internal capacitance of 1 nF; $R_Q = 2.78$ kΩ is calculated as $25/(Q-1)$. The quality factor should be adjusted by setting $Q = R_{Z3}/R_{Z1} = R_{Z3}/R_{Z2}$, which guarantees a pass-band gain of unity. Figure 11 shows the measured frequency response of the transfer function of the 60 Hz notch filter. A reduction of approximately 55 dB is obtained at 60 Hz.

C. Experimental Results

Figure 12 shows the relative sensitivity frequency response between the crosshair PVDF microphone and the PCB 130C10 reference microphone. This measurement was obtained using band-limited random noise of 94 dB with a frequency range up to 20 kHz. The tested bandwidth was limited by the bandwidth of the speaker used in the PWT setup.

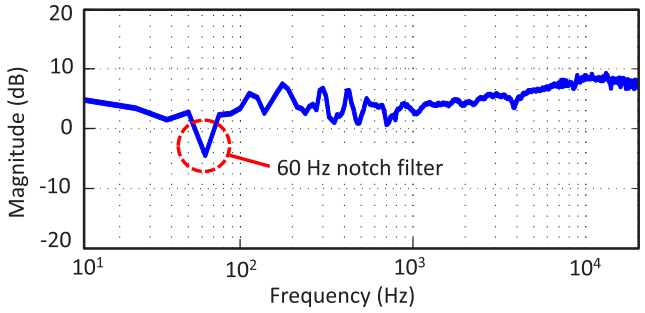

Fig. 12. Relative sensitivity frequency response between the crosshair PVDF microphone and the commercial PCB 130C10 microphone.

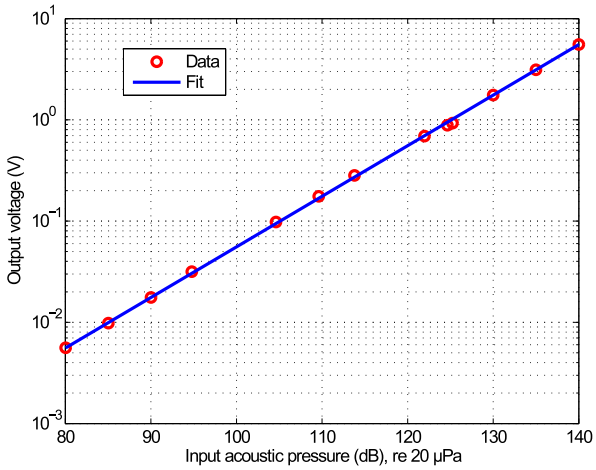

Fig. 13. Measured linearity of the crosshair PVDF microphone at 1 kHz.

The data were obtained by averaging the single-sided auto-power spectral density (PSD) G_{xx} and cross PSD G_{xy} estimates from 20 records of the measured signals. The spectrum, with a frequency resolution of 12.5 Hz, was computed using the Fast Fourier Transform (FFT) algorithm and Hanning window applied to the discrete time domain data. The response has overall fluctuations of less than ±4 dB over the frequency range of 10 to 20,000 Hz, except for the notch frequency of 60 Hz (shown at 62.5 Hz in Figure 12 due to the frequency resolution).

The measured linearity of the microphone at 1 kHz is shown in Figure 13 for sound pressures around the sensitivity calibration pressure of 124 dB. A 1 kHz sinusoidal wave was generated by the DataPhysics Quattro to drive the speaker and excite both the crosshair PVDF microphone and the reference microphone. The linearity plot shows that the crosshair PVDF microphone exhibits an almost linear response (constant sensitivity) up to sound pressures of 140 dB. The maximum sound pressure that could be tested was limited by the output capacity of the speaker. Also, the setup did not have the acoustic and electromagnetic shielding necessary for measuring the noise floor of the microphone.

The sensitivity calibration tests of the microphone were conducted using a 1 kHz sine wave at an SPL of 124 dB. A tube with a diameter of 101.6 mm (4 in) and a length of 1 m was used to propagate a 1 kHz plane wave.

TABLE I

PEAK VALUES OBTAINED FROM THE LINEAR SPECTRA OF THE PVDF MICROPHONE AND THE REFERENCE MICROPHONE FOR TEN TEST RUNS

n	1	2	3	4	5	6	7	8	9	10
V_{CROSS} (V)	1.2124	1.2258	1.2088	1.2729	1.2530	1.2482	1.2624	1.2356	1.2714	1.2624
V_{PCB} (V)	0.8719	0.8658	0.8751	0.9023	0.8928	0.8938	0.9014	0.8919	0.9122	0.9139

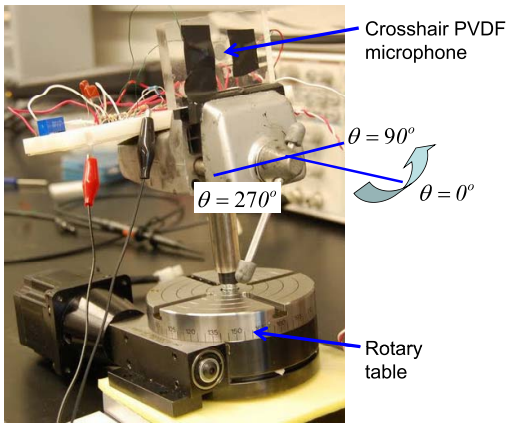

Fig. 14. Experimental setup for characterizing the directivity.

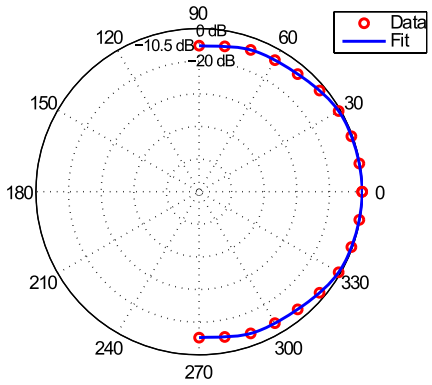

Fig. 15. Measured directivity of the crosshair PVDF microphone.

The linear spectrum was obtained from the data using an FFT and a uniform window. It is noted that for a sinusoidal wave with an amplitude of A, the double-sided linear spectrum will show a spike with a magnitude of A, but that the SPL corresponds to the root mean square (RMS) value $A/\sqrt{2}$. The reference microphone has a sensitivity specification of 19.9 mV/Pa so, to maintain an SPL of 124 dB (i.e., RMS pressure of 31.6979 Pa), the theoretical RMS output voltage of the reference microphone should be 0.6308 V. This RMS voltage corresponds to an amplitude of 0.8921 V (i.e., $\sqrt{2} \times 0.6308$ V) in the linear spectrum. Table I shows the recorded peak values at 1 kHz from the double-side spectra of ten test runs on the two microphones. According to this table, the average sensitivity of the crosshair PVDF microphone is 27.78 mV/Pa or, equivalently, −31.13 dB (re 1 V/Pa) with a standard deviation of 0.24 mV/Pa or 0.074 dB.

From (3), the sensitivity of a flat continuous PVDF film working in 3-3 mode is $K_1 = -g_{33}\ h$, where $g_{33} = -0.330$ V/mN and $h = 28\ \mu$m for MSI PVDF film. Thus, the theoretical sensitivity of MSI PVDF film is 9.24 μV/Pa. For the crosshair PVDF microphone, since the amplifier gain of 1000 is used, the sensitivity of the sensor itself (excluding the amplifier) is 27.8 μV/Pa. Therefore, the sensitivity amplification ratio is 3.01 (27.8/9.24), compared to the physical amplification ratio of 3.2. This small difference may result from neglecting lateral stresses in the theoretical sensitivity of the PVDF film. Because the electrodes are bonded to the rigid substrate and crosshair pattern, stresses applied in the x_3 direction also induce lateral stresses. While the stiffness of the adhesive is unknown, lateral constraints reduce the effective g_{33} coefficient [23] and, consequently, the theoretical sensitivity. As a result, lateral constraints should be minimized in microphone designs. Possible sources of experimental error include fabrication tolerances and signal loss due to the cable capacitance and the input capacitance of the amplifier.

The directivity of the crosshair microphone was measured using the experimental setup shown in Figure 14. A speaker was placed in front of the microphone at a distance of 1 m. The directivity (Figure 15) was obtained by changing the angle of the microphone using a rotary table which rotates from −90 degrees (i.e., 270 degrees) to 90 degrees. A 1 kHz sinusoidal wave was utilized as the excitation wave and the output voltage at 0 degrees was used as the reference. The measurement results in Figure 15 show a decay of about −10.5 dB at ±90 degrees.

VI. CONCLUDING REMARKS

New acoustic sensors with high sensitivity, wide dynamic range, and high frequency bandwidth are needed to address the emerging requirements of many acoustic, aeroacoustic, and clinical applications. This article presents the design, sensitivity modeling, finite element analysis, fabrication, and characterization of a new type of millimeter-size PVDF acoustic sensor based on a crosshair pattern using area ratio amplification and capacitance minimization principles. This acoustic sensor can theoretically achieve 3.2 times the sensitivity of existing commercial PVDF film in combination with a dynamic range of 180 dB and a frequency bandwidth of approximately 100 kHz. Increased sensitivity is achieved through pressure amplification (created by the area ratio between the rigid surface exposed to acoustic waves and the crosshair pattern) in combination with reduced capacitance (created by a patterned top electrode).

Various techniques such as CAD/CAM and FEM are employed for the design and fabrication of the microphone. Finite element simulations including static structure analysis, modal analysis, and harmonic response are performed in ANSYS WORKBENCH to design and analyze the microphone assembly with a requirement of a dynamic range up to 180 dB and a frequency bandwidth of up to 100 kHz.

Three adjacent resonant frequencies, including the fundamental natural frequency, are found through a modal analysis. Peak coalescence is observed from the harmonic response of the device. The analysis of static and dynamic stress distributions ensures the mechanical strength of the microphone. An experimental setup is developed to characterize the microphone using a commercially available PCB microphone as the reference. The theory and design of a circular plane wave tube is presented and signal conditioning circuits, including a preamplifier circuit and a notch filter, are developed. Acoustic tests show that the microphone exhibits a linear response up to an SPL of 140 dB and overall fluctuations of less than ± 4 dB over the frequency range of 10 to 20,000 Hz. The maximum tested SPL and frequency are limited by the output capabilities of the speaker used in the PWT setup. The microphone's measured sensitivity is 27.8 mV/Pa, so the sensitivity of the sensor itself (without the amplifier gain of 1000) is 27.8 μV/Pa. This sensor sensitivity is 3.01 times the sensitivity of bulk PVDF film operating in 3-3 mode, which is close to the physical area amplification ratio of 3.2.

The simple fabrication technique presented in this work, based on chemical etching from commercial PVDF film, could be applied to other problems in which the patterning of electrodes can be used to detect various acoustic, vibratory, fluids, or thermal phenomena.

REFERENCES

[1] *Piezo Film Sensors Technical Manual*, Measurement Specialties Inc., Hampton, VA, USA, Mar. 2008.

[2] Q. X. Chen and P. A. Payne, "Industrial applications of piezoelectric polymer transducers," *Meas. Sci. Technol.*, vol. 6, no. 3, pp. 249–267, 1995.

[3] H. Kawai, "The piezoelectricity of poly (vinylidene fluoride)," *Jpn. J. Appl. Phys.*, vol. 8, no. 7, pp. 975–976, Jul. 1969.

[4] M. Tamura, T. Yamaguchi, T. Oyaba, and T. Yoshimi, "Electroacoustic transducers with piezoelectric high polymer films," *J. Audio Eng. Soc.*, vol. 23, no. 1, pp. 21–26, 1975.

[5] R. Lerch and G. M. Sessler, "Microphones with rigidly supported piezopolymer membranes," *J. Acoust. Soc. Amer.*, vol. 67, no. 4, pp. 1379–1381, 1980.

[6] P. E. Bloomfield, W.-J. Lo, and P. A. Lewin, "Experimental study of the acoustical properties of polymers utilized to construct PVDF ultrasonic transducers and the acousto-electric properties of PVDF and P(VDF/TrFE) films," *IEEE Trans. Ultrason., Ferroelectr., Freq. Control*, vol. 47, no. 6, pp. 1397–1405, Nov. 2000.

[7] T. Dias, R. Monaragala, and M. Soleimani, "Acoustic response of a curved active PVDF-paper/fabric speaker for active noise control of automotive interior noise," *Meas. Sci. Technol.*, vol. 18, no. 5, pp. 1521–1532, 2007.

[8] *Guide to Using Poled PVdF—PVDF Properties and Uses*, Precision Acoustics Ltd., Dorset, U.K. [Online]. Available: http://www.acoustics.co.uk

[9] M. M. D. Ramos, H. M. G. Correia, and S. Lanceros-Méndez, "Atomistic modelling of processes involved in poling of PVDF," *Comput. Mater. Sci.*, vol. 33, nos. 1–3, pp. 230–236, Apr. 2005.

[10] T. Dargaville *et al.*, "Characterization, performance and optimization of PVDF as a piezoelectric film for advanced space mirror concepts," Sandia Nat. Lab., Albuquerque, NM, USA, Tech. Rep. SAND2005-6846, 2005.

[11] D. P. Arnold, S. Gururaj, S. Bhardwaj, T. Nishida, and M. Sheplak, "A piezoresistive microphone for aeroacoustic measurements," in *Proc. ASME Int. Mech. Eng. Congr. Expo. (IMECE)*, New York, NY, USA, 2001, pp. 281–288.

[12] D. P. Arnold, T. Nishida, L. N. Cattafesta, and M. Sheplak, "A directional acoustic array using silicon micromachined piezoresistive microphones," *J. Acoust. Soc. Amer.*, vol. 113, no. 1, pp. 289–298, 2003.

[13] S. Horowitz, T. Nishida, L. Cattafesta, and M. Sheplak, "Development of a micromachined piezoelectric microphone for aeroacoustics applications," *J. Acoust. Soc. Amer.*, vol. 122, no. 6, pp. 3428–3436, 2007.

[14] Z. Wang and L. Liu, "Design and analysis of a PZT-based micromachined acoustic sensor with increased sensitivity," *IEEE Trans. Ultrason., Ferroelectr., Freq. Control*, vol. 52, no. 10, pp. 1840–1850, Oct. 2005.

[15] F. Wang, M. Tanaka, and S. Chonan, "Development of a PVDF piezopolymer sensor for unconstrained in-sleep cardiorespiratory monitoring," *J. Intell. Mater. Syst. Struct.*, vol. 14, no. 3, pp. 185–190, Mar. 2003.

[16] S. Charleston-Villalobos, S. Cortés-Rubiano, R. González-Camarena, G. Chi-Lem, and T. Aljama-Corrales, "Respiratory acoustic thoracic imaging (RATHI): Assessing deterministic interpolation techniques," *Med. Biol. Eng. Comput.*, vol. 42, no. 5, pp. 618–626, 2004.

[17] R. L. H. Murphy, "Method and apparatus for displaying body sounds and performing diagnosis based on body sound analysis," U.S. Patent 6 790 183, Sep. 14, 2004.

[18] M. Toda and M. L. Thompson, "Contact-type vibration sensors using curved clamped PVDF film," *IEEE Sensors J.*, vol. 6, no. 5, pp. 1170–1177, Oct. 2006.

[19] J. Xu, M. J. Dapino, D. Gallego-Perez, and D. Hansford, "Microphone based on polyvinylidene fluoride (PVDF) micro-pillars and patterned electrode," *Sens. Actuators A, Phys.*, vol. 153, no. 1, pp. 24–32, Jun. 2009.

[20] H. S. Tzou and W. K. Chai, "Design and testing of a hybrid polymeric electrostrictive/piezoelectric beam with bang–bang control," *Mech. Syst. Signal Process.*, vol. 21, no. 1, pp. 417–429, Jan. 2007.

[21] A. Selamet and P. M. Radavich, "The effect of length on the acoustic attenuation performance of concentric expansion chambers: An analytical, computational and experimental investigation," *J. Sound Vibrat.*, vol. 201, no. 4, pp. 407–426, Apr. 1997.

[22] M. L. Munjal, *Acoustics of Ducts and Mufflers With Application to Exhaust and Ventilation System Design*. New York, NY, USA: Wiley, 1987.

[23] M. B. Moffet, D. Ricketts, and J. L. Butler, "The effect of electrode stiffness on the piezoelectric and elastic constants of a piezoelectric bar," *J. Acoust. Soc. Amer.*, vol. 83, no. 2, pp. 805–811, 1988.

Jian Xu received the Ph.D. degree from The Ohio State University, Columbus, OH, USA, in 2010, the B.E. and M.E. degrees from Tsinghua University, Beijing, China, in 1998 and 2003, respectively, all in mechanical engineering. His research focused primarily on PVDF-based acoustic sensors for sound measurements at The Ohio State University. As a doctoral student, he has worked on various projects, including the development of an epidural needle insertion simulator, a virtual design tool for piezoelectric actuators, and analysis of an intelligent paint booth air conditioning control system for an automotive plant. He was a recipient of the University Fellowship at The Ohio State University.

Leon M. Headings received the B.S., M.S., and Ph.D. degrees in mechanical engineering from The Ohio State University, Columbus, OH, USA, and the B.A. degree in physics from Goshen College, Goshen, IN, USA. He is currently a Research Associate with the Department of Mechanical and Aerospace Engineering, The Ohio State University, working with Prof. Marcelo Dapino. His research interests include modeling, development, and control of smart material devices and advanced energy systems. Prior to his graduate work, he worked in passenger and light truck tire development at Bridgestone Americas, Inc., Akron, OH, USA.

Marcelo Dapino received the Ph.D. degree in engineering mechanics from Iowa State University, Ames, IA, USA. He is the Honda R&D Americas Designated Chair in Engineering at The Ohio State University, Columbus, OH, USA, where he is a Professor with the Department of Mechanical and Aerospace Engineering. He serves as Associate Director for Research of the Smart Vehicle Concepts Center, a National Science Foundation Industry/University Cooperative Research Center at The Ohio State University, and is a Senior Fellow of the Ohio State University Center for Automotive Research. His research interests include research, development, and manufacture of smart material systems and structures. Prof. Dapino is a Fellow of the American Society of Mechanical Engineers.